Nationaal Lucht- en Ruimtevaartlaboratorium
National Aerospace Laboratory NLR

NLR-TP-2002-193

Design and analysis of stiffened composite panels for damage resistance and tolerance

J.F.M. Wiggenraad, E.S. Greenhalg and R. Olsson

Nationaal Lucht- en Ruimtevaartlaboratorium
National Aerospace Laboratory NLR

NLR-TP-2002-193

Design and analysis of stiffened composite panels for damage resistance and tolerance

J.F.M. Wiggenraad, E.S. Greenhalg* and R. Olsson**

* QinetiQ, Farnborough, United Kingdom

** FOI-Swedish Defence Research Agency, Stockholm, Sweden.

This report is based on a presentation held at the Fifth World Congress on Computational Mechanics, Vienna, Austria, 7-12 July 2002.

Customer:	National Aerospace Laboratory NLR
Working Plan number:	S.1.A.3
Owner:	National Aerospace Laboratory NLR
Division:	Structures and Materials
Distribution:	Unlimited
Classification title:	Unclassified
	May 2002

Contents

(14 pages in total)

Design and Analysis of Stiffened Composite Panels for Damage Resistance and Tolerance

Jaap F.M. Wiggenraad*

National Aerospace Laboratory, NLR
P.O. Box 153, 8300 AD Emmeloord, The Netherlands
e-mail: wigg@nlr.nl

Emile S. Greenhalgh

QinetiQ
Room 2008, A7 Building, Farnborough, GU14 0LX, United Kingdom
e-mail: esgreenhalgh@qinetiq.com

Robin Olsson

FOI-Swedish Defence Research Agency, Aeronautics Division FFA
SE-172 90 Stockholm, Sweden
e-mail: robin.olsson@foi.se

Key words: composite materials, stiffened panels, damage tolerance, damage resistance, preliminary design

Abstract

This paper describes a joint Dutch-Swedish-British programme for reducing the effect of impact on skin-stringer composite panels. An optimisation code for the design of such panels was extended with the capability to optimise panels for “damage resistance”. Hereto, a damage initiation constraint was implemented. Three different panels were designed, fabricated and tested: one baseline configuration with previous design methodology, and two “damage resistant” configurations, according to the new design capability. The new criterion was found accurate for impacts at stiffener foot locations, and conservative for impacts at midbay locations between stiffeners. Although the panels were not fully damage resistant for 35 J impacts as intended, the results were close, and clearly superior to the baseline configuration. The penalty for increased damage resistance is increased panel weight, while the advantages are savings of fabrication and maintenance costs. Delamination growth after impact was simulated with a moving mesh FE-model. The simulations demonstrated a strong interaction between global skin buckling and the location and growth of delaminations. Delamination growth is promoted by location at a buckle crest and retarded by location at a node line.

1 Introduction

Although aircraft structures made of composite materials may have superior properties, compared to metal structures, when considering structural weight, corrosion resistance and fatigue behaviour, they are more vulnerable to defects incurred during production, or damage induced during service. Impact damage or defects, when present in composite structures, are known to reduce the strength considerably, in particular the compression strength, because the highly loaded fibres are no longer adequately supported by the matrix. Moreover, the presence of defects, or the extent of impact damage are difficult to detect, and the residual strength of the flawed or damaged structure is difficult to predict. As structures must still be able to carry the ultimate design load, even when containing "barely visible impact damage", these technological problems result in conservative designs, time consuming inspection procedures and expensive repair techniques. For instance, the industry is designing aircraft structures based on a "no-growth" requirement for damage, which is more stringent than the equivalent concept for metal structures, i.e., allowing a certain tolerance of crack growth.

Considerable efforts have been undertaken to make composite structures more damage tolerant, i.e., to minimise the strength reduction caused by the presence of a specified defect, or resulting from a specified impact threat. Meeting this objective has been pursued by improving materials systems and by optimising geometric configurations, with modest success, and often at the price of increased production costs. More recently, efforts have been aimed at the design of composite structures which are not just more damage tolerant, but also more damage resistant. This would lead to a saving of costs associated with inspection and repair, and of fabrication costs, but also to increased structural weight. Clearly, to obtain structural designs with improved damage tolerance and resistance, while minimising cost and weight penalties, a design optimisation procedure is required. Such a procedure depends on reliable predictions of the buckling load, of the impact energy at which damage will be incurred, and of the load at which damage will grow. These predictions must be carried out numerically, based on models that are sufficiently simple to be used at the design level. Moreover, prediction methods must be validated against experimental results, which demonstrate the overall structural behaviour, as well as the relevance of damage models used for design purposes.

The development of such a capability has been undertaken in a joint research programme carried out by a tri-national consortium of the aerospace research establishments of the Netherlands (NLR), the UK (QinetiQ), and Sweden (FOI), and was sponsored by the respective Ministries of Defence. The acronym of the programme is DAMOCLES: "DAmage Management Of composite structures for Cost effective, Life-Extensive Service". The research centres used complementary capabilities to achieve this goal: the extension of a design optimisation code with a constraint for impact damage initiation by NLR, the development of a damage growth prediction capability by FOI, and the experimental validation and failure analysis by QinetiQ.

The approach followed consisted of a sequence of activities. Initially a survey was done of impact threats, as well as design practice and demands of the aircraft industry in the three countries [1]. The survey stressed the need for increased design strains and reduced life cycle costs. With the extended optimisation code, three different panel designs were obtained: one design, the *baseline* configuration, without considering the damage initiation constraint, and two other configurations with an increased level of damage resistance. Several panels were fabricated for each configuration, and the impact energy level, at which damage was initiated, was established experimentally, to validate the damage initiation criterion used in the optimisation code. Subsequently, panels for each configuration were impacted with the same amount of impact energy, and tested by in-plane, longitudinal compression, eventually up to failure. The load levels, at which buckling induced delamination growth was taking place were established, and compared to the predicted values. Similarly, the overall buckling and failure loads of the panels were evaluated. Ultimately, the results were evaluated with respect to the aims set out at the beginning of the programme.

2 Design optimisation

To achieve a minimum weight design, the design optimisation code PANOPT [2] finds optimum values for a range of selected design variables, while satisfying a set of specified constraints. Design variables used in the present study were ply thicknesses for given laminate stacking sequences, and geometric entities, such as

stiffener dimensions and the stiffener pitch. The constraints that were imposed are limits on buckling loads, overall panel stiffness, geometric dimensions, etc., as well as a newly developed "damage initiation constraint". At each optimisation cycle, the constraints of the current design were evaluated to determine whether they were active, inactive or violated. This required the performance of appropriate numerical analyses, such as the calculation of the buckling load of the panel, or the peak force that would occur during an impact on the panel at a specified energy level. Upon this evaluation, certain design variables were changed, until a minimum weight design was achieved which satisfied all constraints.

A previous study [3] carried out at NLR was aimed at the design of damage tolerant stiffened, composite panels by numerical optimisation, for which a multi-model capability was developed, and incorporated in the computer code PANOPT. This capability allows the design optimisation process to consider several configurations simultaneously, representing the panel in an undamaged state, as well as in several representative damage states, each for different strength criteria, depending on the severity of the damage. This study indicated that the multi-model approach clearly results in different, lighter panel configurations than when such scenarios are considered one by one. As already postulated in [3], the same multi-model capability can also be used to design panels, which are more "damage resistant", i.e., panels that will not be damaged in case they are impacted at a certain maximum energy level. To facilitate the design of panels for damage resistance, the optimisation code PANOPT, which uses an efficient finite strip analysis routine [4] to compute buckling loads, and a corresponding finite element representation to compute deflections, was extended with a new "damage constraint", based on an impact damage initiation criterion.

The impact damage initiation criterion used [5] is based on the observation that the maximum value of the force, exerted during an impact, determines whether delamination will or will not be induced. The damage initiation criterion as implemented in the design optimisation code PANOPT by defining a critical force F_{cr} for delamination initiation:

$$F_{cr} = \tfrac{1}{3}\pi\, t^{3/2}\sqrt{8G_{IIc}E\big/\left(1-\nu^2\right)} \tag{1}$$

where t is the laminate thickness, G_{IIc} is the critical strain energy release rate in mode II delamination and E and ν are the average elastic constants of the laminate [5]. If it is assumed that the structural response during the impact is linear elastic up to delamination initiation, the force-deflection "curve" is a straight line, and the triangular area below the curve represents the impact energy.

If the impact threat, for which damage resistance must be "guaranteed", is specified as a critical amount of energy (E_{cr}) below which damage may not occur, the critical minimum displacement that the structure must allow is given by:

$$d_{cr} \geq 2E_{cr}/F_{cr} = 6E_{cr}\Big/\left(\pi\, t^{3/2}\sqrt{8G_{IIc}E\big/\left(1-\nu^2\right)}\right) \tag{2}$$

A structure made of a more brittle material, i.e., a material with a smaller value of G_{IIc}, must allow more displacement, i.e., has to be more flexible.

The peak force is determined in PANOPT by computing the transverse displacement resulting from an applied unit force, and scaling up the force, hence the displacement, until the work done by the force is equal to the specified maximum impact energy. If the damage initiation constraint is violated, either the critical peak force must be increased by increasing the plate thickness, or the deflection occurring at the maximum energy must be increased by decreasing the transverse panel stiffness, for instance, by enlarging the stiffener pitch. Clearly, the impact damage initiation prediction is based on static, linear analysis. However, it was shown in various studies, that static indentation may give similar damage as low velocity impacts, such as caused by tool drops, which are the threats considered here. In a more detailed, non-linear finite element analysis, it was shown that the use of linear theory may result in the overestimation of the deflection of typically ten percent for the configurations and impact energy considered in the present study [6].

3 Panel design

Although ply angles may be selected in PANOPT as design variables, the design variables specified in the optimisation process were ply thicknesses (rounded up in a second design cycle to integer ply numbers) and geometric entities. As ply angles and stacking sequences are usually selected a priori because of a wide range of constraints, they were not considered by PANOPT. As changing material properties is not practical, for the optimisation process to find designs with an increased impact resistance, either the transverse flexibility must be increased (by increasing the stiffener pitch, for instance), or the local laminate thickness must be increased by increasing one or more ply thicknesses. It is obvious that a damage resistant panel carries a weight penalty compared to designs derived without damage constraints, but the objective of the optimisation is to keep the weight penalty to a minimum.

Three different I-stiffened panels were designed for a running load of 1500 N/mm (design ultimate load) and a length of 550 mm with the following constraints:

Minimum Euler buckling load	1800 N/mm
Minimum torsional buckling load	1800 N/mm
Minimum local skin buckling loads	1800 N/mm
Maximum postbuckling strain ratio	1.25 at 1800 N/mm
Minimum axial panel stiffness	$\varepsilon < 0.006$ at 1500 N/mm

Minimum stiffener pitch, and minimum and maximum stiffener dimensions.

The buckling loads were given a safety factor of 1.2, to compensate for the possibility that different buckling modes might coincide. Based on previous experience, the postbuckling strain ratio (postbuckling strain range divided by pre-buckling strain range) was limited to 1.25, to prevent postbuckling to occur below design limit load (1000 N/mm). The panel stiffness was constrained by an empirical value (maximum strain of 0.006 at design ultimate load), to provide sufficient damage tolerance, and geometric constraints were based on practical considerations, related to fabrication issues. The laminate stacking sequence was defined a priori, based on design rules.

The first design was the baseline design (BL), for which the newly developed damage initiation constraint was *not* considered. For the second and third designs, the damage initiation constraint was considered, i.e., they were required to be damage resistant designs (DR1 and DR2). The DR2 design was constrained to have a larger stiffener pitch than the DR1 design, to further drive down the manufacturing costs. Stiffener pitches for the three optimised designs were 150 mm, 179 mm, and 250 mm, respectively. The impact scenarios considered for the second and third designs were an impact at a midbay location between stiffeners, and an impact at the stiffener foot location, both at 35 J (Fig. 1). The latter impact location turned out to be a design driver for both DR1 and DR2 designs. Considering the damage resistance criterion during the optimisation resulted in weight penalties compared to the baseline configuration (7.9 kg/m²) of 16% and 28% for DR1 and DR2, respectively. The resulting designs are shown in Fig. 2.

The computed performance of the three panel designs is shown in Fig. 3. The active constraints of the BL design are the minimum pitch, maximum stiffener top and foot widths, and local buckling, while the torsional buckling strength was actually somewhat violated at 1645 N/mm. The active constraints of the DR1 design are maximum stiffener foot width, damage initiation at the stiffener edge, and Euler buckling. The active constraints of the DR2 design are maximum stiffener top and foot width, damage initiation at the stiffener edge, Euler and local buckling, while the torsional buckling constraint was accidentally violated at 1072 N/mm. Although the panels were designed for a length of 550 mm, representing a typical rib pitch, they were eventually tested at a length of 450 mm, the ends embedded in 15 mm thick epoxy blocks. Hence, the torsional buckling load, which is inversely proportional to the panel length, was not as critical in the tests.

4 Impact damage

Of each of the three configurations, three test panels were fabricated, using Hexcel IM7/8552 prepreg material. One panel of each of the configurations was used to determine the actual impact damage threshold, in terms of impact energy, i.e., the *damage resistance*. Using an instrumented drop weight impactor, with a mass of 2.312

kg, and a diameter of 12.7 mm, impacts were applied at several midbay and stiffener foot (edge of stiffener) locations (Fig. 1) at different energy levels. The damage extent was determined by C-scan, and further post-failure analysis was carried out at FOI to support the development of their damage growth prediction capabilities.

The impact energy level corresponding to damage initiation was established at less than 15 J for the baseline configuration (BL), 25 J for panels DR1 and DR2 impacted on a stringer foot, 30 J for panel DR1 when impacted in a midbay position, and more than 40 J for a midbay impact on panel DR2 (Fig. 4a-c). This implies, that damage resistance for 35 J impacts was not fully met for the DR1 and DR2 designs, i.e., damage resistance is achieved for 25 J only. However, for design purposes, the trend was clearly predicted: improved damage resistance being achieved with increased stiffener pitch and skin thickness. Moreover, the predicted peak forces initiating damage were well in accordance with the critical peak force given by Eq. 1 [7].

Later, the remaining six panels, i.e. two BL, two DR1 and two DR2, were impacted at 35 J (Fig 4d), either at a midbay or at a stiffener foot location, to establish the *damage tolerance* of each of the three designs for equal impact threats, by loading them to failure in compression.

5 Compression tests

After impacting, the panels were prepared for compression testing by mounting in resin blocks, to avoid brooming of the ends, and reduced in length to 450mm to avoid any buckle mode interactions. The panel sides were also cropped to avoid any unrealistic free-edge buckling. A complete description of the tests is given in [8]. The panel instrumentation is shown in Figure 1; the gauges shown in grey (red) were averaged to determine the applied strain on the panel. LVDTs monitored out-of-plane deflections. Buckling of the panel was defined as when back to back gauges in the bays exhibited significant divergence (*i.e.* large bending strains). Prior to testing, the front faces of the panels were lightly abraded and sprayed white, to facilitate Moiré interferometry. During testing a coarse grating (one line/mm) was placed on the front face to capture the buckling and larger out-of-plane displacements. This was illuminated from an angle of about 25°; each fringe corresponded to an out-of-plane displacement of about 2mm.

Prior to impacting, one panel of each type was compressively tested to just above design limit load (DLL) to validate the buckling predictions. Subsequently, the panels were impacted and tested to failure. Initial tests were in quasi-static compression in a Schenck 1000 kN servo-hydraulic test frame, in displacement control at a rate of 1mm/min. However, for the DR1 and DR2 panels, the strength exceeded the capacity of the test machine, and they were then tested in an Amsler 2000 kN servo-hydraulic test frame. Unfortunately, cracks developed in the end-blocks of some of the panels, leading to premature failure. After testing to failure, the panels were analysed using fractographic techniques to determine the failure processes. The results of the tests are shown in Table 1. It should be noted that two panels failed at the end-blocks. These panels were C-scanned to characterise any damage growth from the impact site but none was found.

Results from the BL panels; both the undamaged and bay damaged panels buckled in three half waves (Figure 5a) at an applied strain of about –2400με. As the load increased the buckling of the bay containing damage started to change slightly (Figure 5b); flattening and extending laterally towards the stringers at a strain of -5000με. At an applied strain of –5400με, there was a small jump in the data and failure then occurred at an applied strain of -5945με (-798 kN), which was 132% of DUL. The foot damaged panel buckled at a slightly lower strain (-2300με) but the buckle mode was the same; three half waves. At an applied strain of -3850με, there was a significant event in the results with a large drop in strain over the central stiffener. Failure then occurred at applied strain of -4339με (-680 kN); 96% of DUL. These results indicate that the predicted and actual panel buckling were close (approximately -2400με), and the presence of the impact promoted panel buckling slightly. The presence of bay impact did not bring the strength below DUL (-4500με) but the foot impact (which had a greater damage extent) did reduce the strength to below DUL.

Results from the DR1 panels; the introduction of impact damage did not change the buckling strain (-2700με) or mode (two half-waves in the bay) of the DR1 panels (Figure 6). There was no evidence of damage growth in the panels up to failure/stopping the test at -4630με (-1012 kN) and -4573με (-1004 kN) for the bay and foot impacts respectively; about 124% of DUL. Note that these values should be considered a lower bound on the strength since the bay panel failed through end-block failure whilst the foot impact exceeded the test machine capacity

and had not been tested to failure. As with the BL designs, the predicted and actual panel buckling were close (approximately -2700με), but the presence of impact had no effect on panel buckling. However, unlike the BL design, the presence of impact (either in the bay or foot) did not bring the strength below DUL (-3700με), although it should be noted that the damage extent was significantly less than that in the BL designs.

Results from the DR2 panels; the introduction of impact damage led to large changes in the buckling strains from –1700με in the undamaged panel although the buckle mode did not change; single half-waves in each bay (Figure 7a). In the bay impact panel it dropped to 82% (–1400με) whilst in the foot impact panel it increased to 118% (-2000με). As the load increased further, the buckle mode switched to two half waves in the bay (Figure 7b), The switch occurred at a strain of -2750με for the undamaged panel, at -3200με for the panel with bay impact and –2300με for the panel with foot impact. For the bay impact there was some evidence of initiation of failure at -4400με, with final failure occurring at an applied strain of -4699με (-1190 kN); 112% of DUL. For the foot impact there was no evidence of damage growth prior to failure which occurred at an applied strain of -3792με (-1005 kN); 90% of DUL. Failure was observed to have been due to end-block failure. For the DR2 designs, the predicted and actual panel buckling strains were close (approximately -1700με), but the presence of impact had a large effect on the panel buckling. The impact damage in the bay was negligible and the panel exceeded DUL. For the impact in the foot, although the failure was below DUL (-4200με), it should be noted that the measured strength was a lower bound due to end-block failure occurring.

Table 1 Overview of experimental results

Panel type	Impact	Design buckling strain [με]* L=550 mm	Design Ůat DUL	P at DUL [kN]	Test buckling strain [με]* L=450mm	Test Ůat failure [με]	Test failure load [kN]	Failure mode	Damage area [mm²]
BL W=0.4 m	Bay	2482 (4)	4500	600	2400 (3)	5945	798	Failed	881
	Foot	2482 (4)	4500	600	2300 (3)	4339	680	Failed	1118
	No	2482 (4)	4500	600	2400 (3)	3848	616	Stopped	-
DR1 W=0.46 m	Bay	2784 (3)	3700	687	2700 (2)	4630	1012	End-block	697
	Foot	2784 (3)	3700	687	2700 (2)	4573	1004	-	872
	No	2784 (3)	3700	687	2700 (2)	2936	711	Stopped	-
DR2 W=0.6 m	Bay	1815 (2)	4200	900	1400 (2)	4699	1190	Failed	0
	Foot	1815 (2)	4200	900	2000 (2)	3792	1005	End-block	639
	No	1815 (2)	4200	900	1700 (2)	3566	945	Stopped	-

*) Numbers in brackets indicate number of half waves

6 Simulation of delamination growth with buckling

The buckling and resulting delamination growth in the impacted panels was simulated by FOI with an in-house FE-based code, DEBUGS [9]. In this code growth of single delaminations is simulated by use of a moving mesh, where growth is governed by a fracture mechanics criterion, accounting for local and global buckling and contact between the substrate and the delaminated sublaminate. The geometrically nonlinear FE-analysis is done iteratively using a shell element model in the commercial code ADINA. Within the programme the structural model in DEBUGS was extended from plain panels to stiffened panels [10]. A model example is given in Fig. 8.

The code includes an approximate mode separation and a mixed mode growth criterion. However, based on previous analyses a mixed mode ratio of G_I/G_{II}å1 and a corresponding delamination toughness of G_c=350 J/m^2 was assumed in the present analysis.

Only mid-bay impact damage was modelled since the present version of the code is unable to model delamination growth under stiffeners. The impact damage was represented by single elliptical delaminations with the major axis in the load direction. Based on ultrasonic C-scans [8] the following delamination sizes were

assumed: 42x30 mm for the BL panel, 40x32 mm for the DR1 panel and 34x28 mm for the DR2 panel. For each panel a number of interfaces were scanned to find the most critical depth for delamination growth.

In a preliminary analysis of the designed geometries it was noted that the skin buckling modes were sensitive to delamination depth and other small changes in geometry [11]. In some cases a buckling mode switch ("snap-through") was predicted. This sensitivity was reflected in a poor agreement between predicted and measured deflection modes for the finally tested geometry, although buckling strains and buckling loads were in fairly good agreement, Table 2 [12]. Interfaces with experimentally observed delamination growth are taken from the fractographical study in [8]. Furthermore, delamination growth was found to be highly dependent on whether the damage was located on a node line or in a skin buckling crest. As expected, delamination growth was promoted at buckling crests, where large bending strains are superimposed on the applied membrane strain. Note that delamination growth is predicted below the same sub-laminate for both DR1 and DR2, although the predicted onset strain is much higher for a delamination at a node line (2 buckles). The switch from 1 to 2 buckles in DR2 appears to explain the lack of delamination growth in this panel.

Homogenisation of the thicker substrate was found to cause fairly large errors in the buckling load for the BL panels, while the effect was small for the thicker DR1 and DR2 panels. Furthermore, neglect of the unidirectional filler in the "Bermuda triangle" caused a severe underestimation of the buckling load for all three panels, in spite of correct buckling strains. Inclusion of this material improved predictions significantly. Table 2 gives a comparison of test results and predictions by models with the filler and all layers included.

Table 2 Comparison of DEBUGS predictions and experimental results

Panel type	Result	Interface	Skin buckling		Delamination growth		Number of buckles
			Load [kN]	Strain [%]	Load [kN]	Strain [%]	
BL	Predicted	3/4 or 4/5	397	0.20	825	0.46	2
	Experiment	*4/5*	*433*	*0.24*	*631-720*	*0.40-0.50*	*3*
DR1	Predicted	4/5	700	0.26	1665	0.80	2
	Experiment	*No growth*	*670*	*0.27*	*>1012*[a]	*>0.46*[a]	*2*
DR2	Predicted	4/5	560	0.16	694	0.21	1
	Exp. 1st mode	-	*494*	*0.17*	-	-	*1*
	Exp. 2nd mode	*No growth*	*775*	*0.28*	*>1190*[b]	*>0.47*[b]	*2*

[a] End-block failure [b] Skin compression failure without delamination growth

7 Conclusions and recommendations

An optimisation code for the design of stiffened, composite panels was extended with the capability to optimise panels for “damage resistance”. Hereto, a damage initiation constraint was implemented, based on a critical peak force. The critical peak force is the discriminator between impacts which do or do not result in impact damage.

Three different composite stiffened panels were designed: one baseline configuration with previous design methodology, and two “damage resistant” configurations, according to the new design capability. Panels were fabricated and impacted, and the peak forces were measured to evaluate the damage initiation criterion. This criterion was found to be accurate for impacts at stiffener foot locations, and somewhat conservative for impacts at locations midbay between stiffeners.

The panel optimisation was carried out in an early stage of the project, based on several non-conservative assumptions. Although the panels were not fully damage resistant for 35 J impacts as intended, the results were close, and clearly superior to the baseline configuration. Impacts at stiffener foot locations were driving the design, while impacts at midbay locations were not. This suggests that improvement of the skin-stiffener interface area will lead to a higher degree of damage resistance.

The penalty for increased damage resistance is increased panel weight (16 - 28%), while the advantages are savings of fabrication and maintenance costs. In practice, the weight penalties will not be as large as for the present, fully optimised panels, due to the many other boundary conditions that are imposed during the integration of panels in a structure.

The general failure sequence in the panels started as fairly shallow delaminations extending from the impact damage. Whether the delamination growth across the bay was close to the front (skin) or back (stiffener) faces was controlled by the buckling mode of the panel. Upon reaching the stiffeners, the buckling forces led to the development of deep gouges within the skin, and these gouges facilitated migration of the delaminations to deeper interfaces containing 90° plies. Once within these preferential interfaces, rapid delamination growth occurred, leading to stiffener detachment and catastrophic skin failure through bending/compression.

The main conclusion of the delamination growth simulation was the strong interaction between damage location and skin buckling mode. In general growth was promoted for delaminations located at a buckling crest, and retarded for delaminations on a node line. Thus, the results for the three panels are not fully comparable, since identical impact locations were selected in spite of differences in buckling modes. In practice, the impact location is arbitrary and each panel must fulfil the requirements for all possible locations. It should also be stressed that predicted and observed buckling modes may differ due to geometrical errors, initial imperfections an insufficient description of the boundary conditions. For these reasons it appears that future designs and tests should be based on delaminations in the worst possible location of the respective buckling modes.

Acknowledgements

This investigation was carried out under contracts awarded by the Scientific Research Division of the Directorate of Material, Royal Netherlands Air Force, The Swedish Defence Materiel Administration and the UK Ministry of Defence Corporate Research Programme.

References

[1] R. Olsson, DAMOCLES Task 1-Deliverable: *A survey of impact conditions relevant in aircraft structures*, FFAP H-1353, FFA, Bromma, Sweden., 1998.

[2] P. Arendsen, H.G.S.J. Thuis, J.F.M. Wiggenraad, *Optimisation of composite stiffened panels with postbuckling constraints*, Proc. CADCOMP 94, Southampton, 1994, (also NLR TP 94083, 1994).

[3] J.F.M. Wiggenraad, P. Arendsen, J.M. da Silva Pereira, *Design optimization of stiffened composite panels with buckling and damage tolerance constraints*, Proc. 39th AIAA-SDM Conference, Long Beach, USA, 1998, (also NLR TP 98024, 1998).

[4] E. Riks, *Buckling and post-buckling analysis of stiffened panels in wing box structures*, Int. J. Solids and Structures, 37, (2000) 6795-6824.

[5] G.A.O. Davies, X. Zhang, *Impact damage prediction in carbon composite structures*, Int. J. Impact Eng., 16, (1995), 149-170.

[6] A.L.P.J. Michielsen, J.F.M. Wiggenraad, *Optimisation methodology and discrete designs of wing panels with increased damage resistance*, NLR CR 98621.

[7] J.F.M. Wiggenraad, R.W.A. Vercammen, P. Arendsen, L.C. Ubels, *Design optimisation of stiffened composite panels for damage resistance*, Proc. 41st AIAA-SDM Conference, Atlanta, USA, 2000, (also NLR TP 2000-023, 2000).

[8] E.S. Greenhalgh, *Mechanical evaluation of CFRP skin-stringer panels designed for impact damage tolerance*, DERA/MSS/MSMA2/TR002084.

[9] K.-F. Nilsson, L.E. Asp, J.E. Alpman, L. Nystedt, *Delamination buckling and growth for delaminations at different depths in a slender composite panel*, Int. J. Solids and Structures, 38 (2001) 3039-3071.

[10] S. Singh, L.E. Asp, K.-F. Nilsson, J.E. Alpman, *Development of a model for delamination buckling and growth in stiffened composite structures*, FFA TN 1998-53, FFA, Bromma, Sweden., 1998.

[11] L. Asp, *Preliminary analysis of DAMOCLES panels*, FFAP H-1412, FFA, Bromma, Sweden., 1999.

[12] L. Asp, *Effects of code and geometry corrections on the DAMOCLES analysis results*, FFAP H-1427, FFA, Bromma, Sweden, 2000.

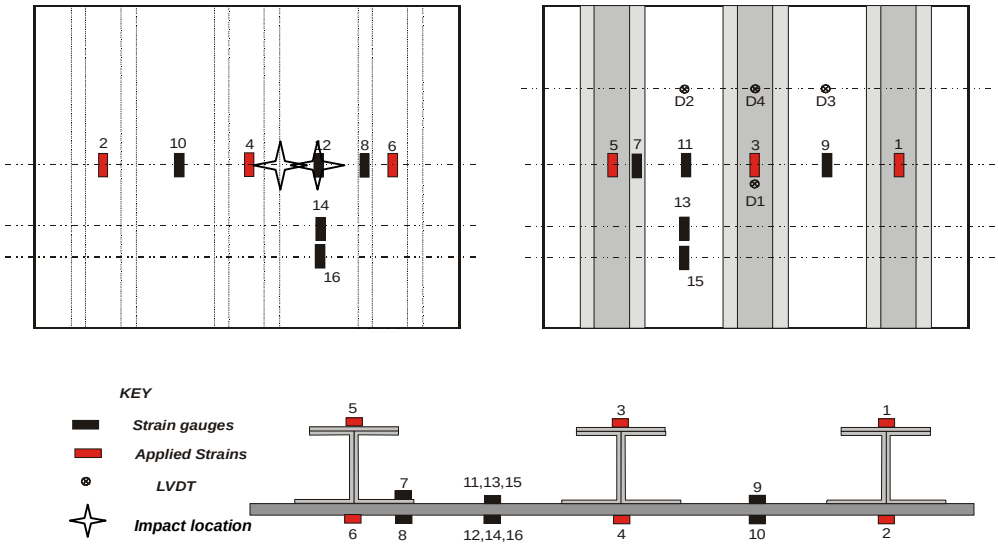

Figure 1 - Impact locations and instrumentation of the panels

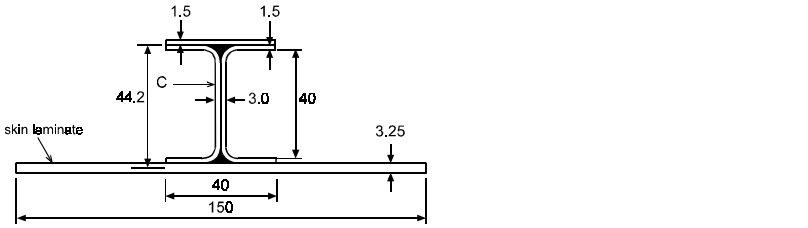

Skin laminate:	[8/16/2] fabricated	: $[45, 0, -45_2, 0, 45, 90, 45, 0, -45_2, 0, 45]_s$	t = 3.25 mm
C-laminate:	[6/4/2]	$[-45, 45, 0_2, 90, 0]_s$	t = 1.5 mm

a) PANOPT model Baseline BL

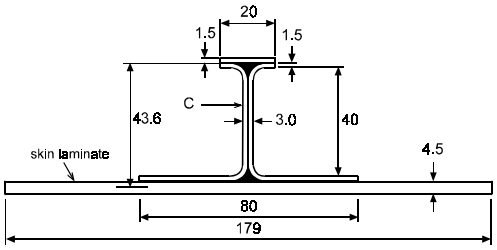

Skin laminate:	[12/20/4]	: $[45, 0, -45_2, 0, 45, 90, -45, 0, 45_2, 0, -45, 90, 45, 0, -45, 0]_s$	t = 4.5 mm
C-laminate:	[6/4/2]	: $[-45, 45, 0_2, 90, 0]_s$	t = 1.5 mm

b) PANOPT model DR1

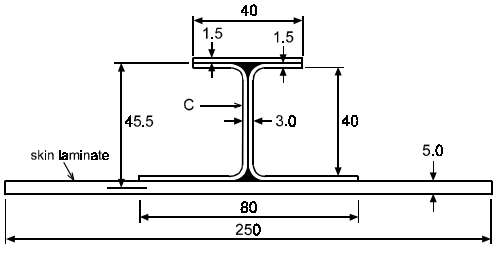

Skin laminate:	[12/24/4]	: $[45, 0, -45_2, 0, 45, 90, -45, 0, 45]_{ss}$	t = 5.0 mm
C-laminate:	[6/4/2]	: $[-45, 45, 0_2, 90, 0]_s$	t = 1.5 mm

c) PANOPT model DR2

Figure 2 – PANOPT design for damage resistant panels

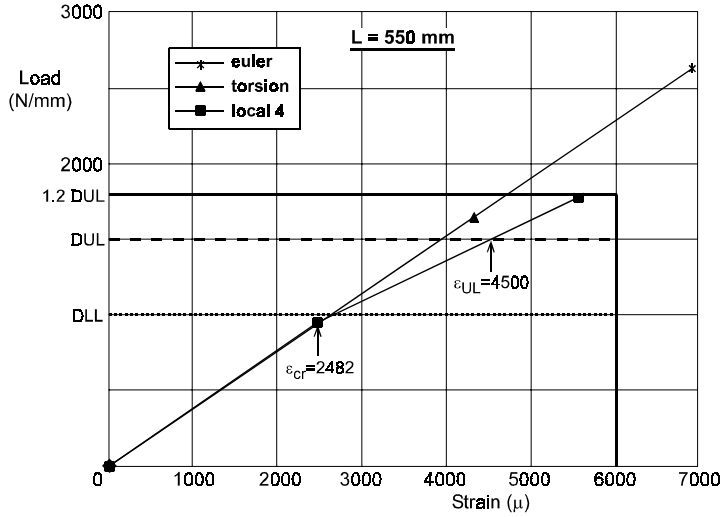

a) Calculated buckling behaviour of baseline panel BL, pitch 150 mm

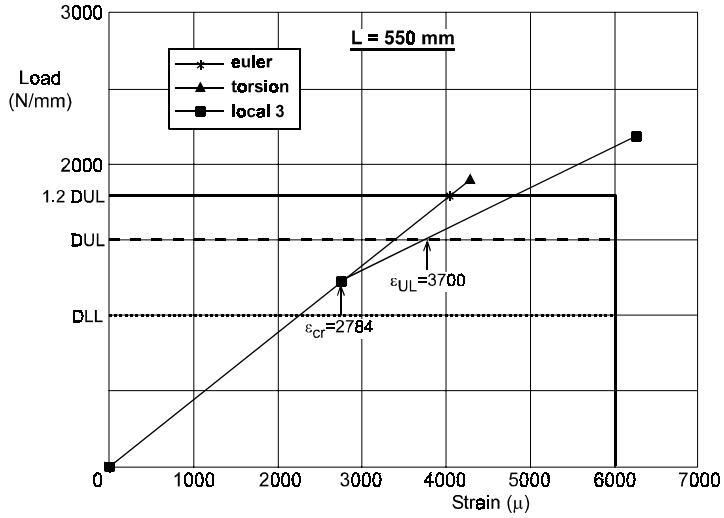

b) Calculated buckling behaviour of damage resistant panel DR1, pitch 179 mm

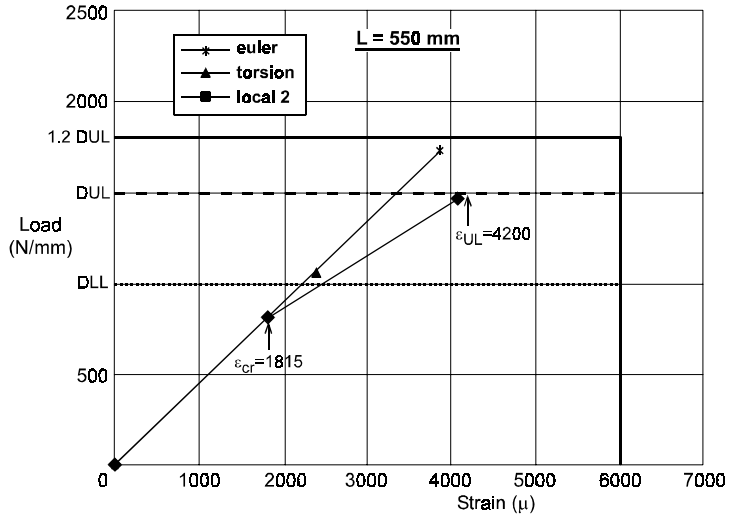

c) Calculated buckling behaviour of damage resistance panel DR2, pitch 250 mm

Figure 3 – Calculated buckling behaviour of the panels

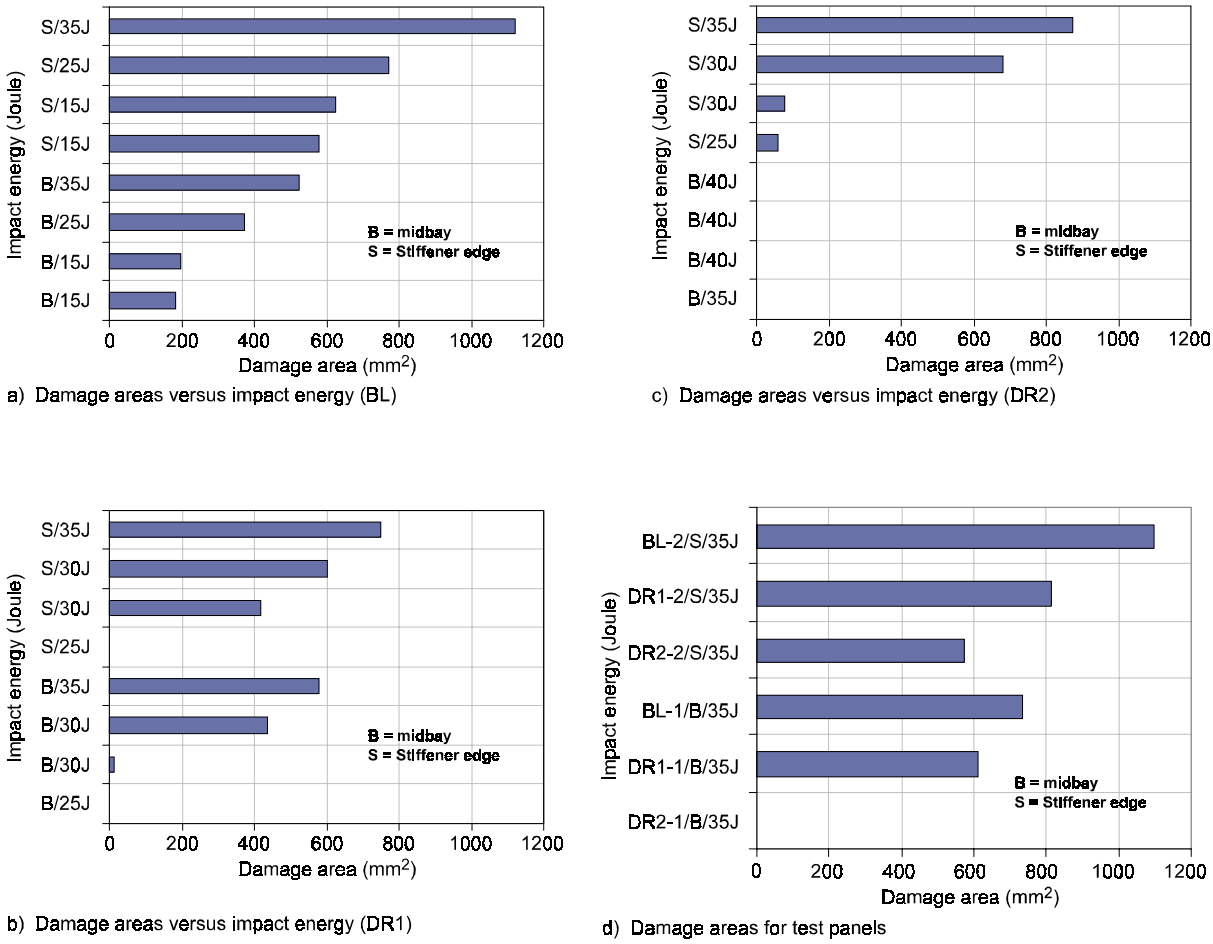

Figure 4 – Damage areas of the test panels

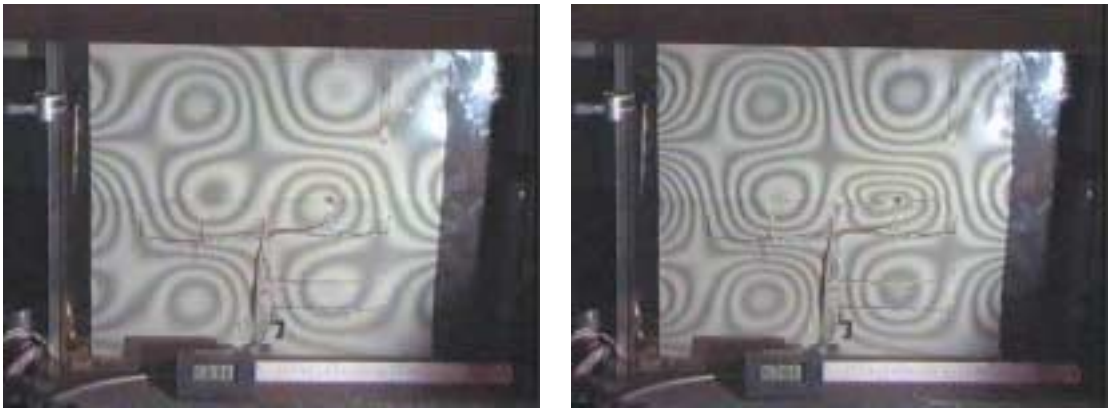

(a) -4040με (b) -5600με

Figure 5 – Front face Moiré of BL after bay impact

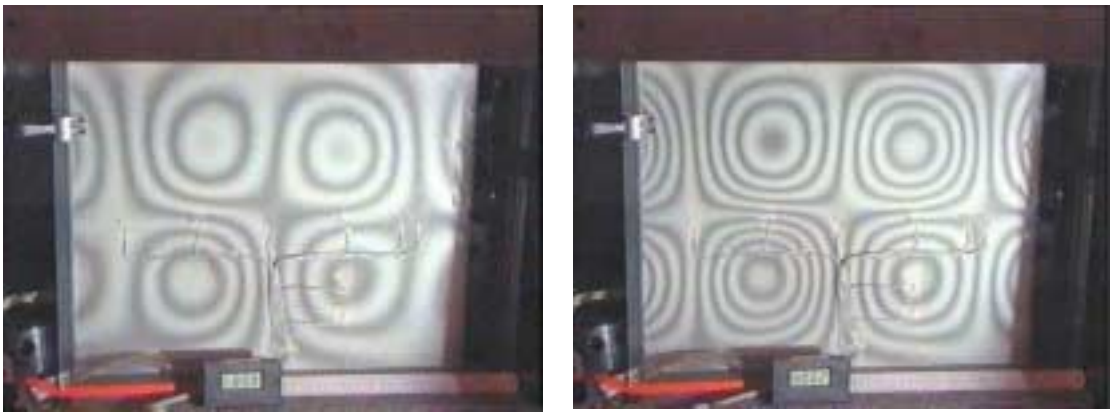

(a) -3400με (b) -4630με

Figure 6 – Front face Moiré of DR1 after bay impact

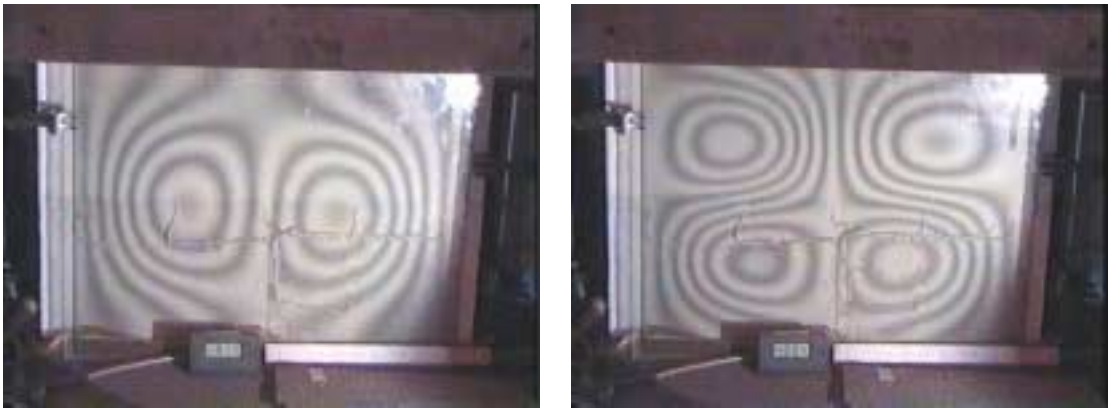

(a) -2800με (b) -3870με

Figure 7 – Front face Moiré of DR2 after bay impact

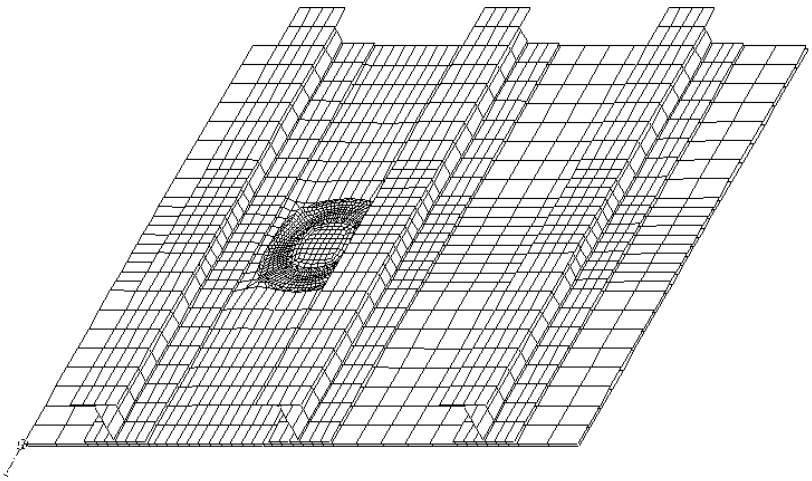

Figure 8 – FE-model of a panel with a mid-bay delamination after local buckling